Generation of cellulose from Saccharum officinarum pseudostem bagasse and its application as solubility enhancer in albendazole solid formulation

Didacus Nnamani*[1], Mumuni Momoh[2], Sam Esezogbo[1]

[1]Department of Pharmaceutics and Pharmaceutical Technology, College of Pharmacy, Igbinedion University Okada, Edo State, Nigeria.

[2]Department of Pharmaceutics, Faculty of Pharmaceutical Sciences, University of Nigeria Nsukka.

Submitted: 6th April, 2023; Accepted: 16th May, 2023; Published: 30th June, 2023
DOI: https://doi.org/10.54117/jcbr.v3i3.7
**Corresponding author: didacus nnamani; nnamani.didacus@iuokada.edu.ng*

Abstract

Formulations of poorly aqueous soluble drugs in different polymers based on solid dispersion method have been used to improve its solubility and drug bioavailability. The aim of this study was to formulate albendazole solid dispersion utilising cellulose obtained from *saccharum officinarum* pseudostem bagasse and characterised. Herein, a 3^2 factorial design was used to factor out 9 combinations of the generated cellulose (GC) and lactose. In each case, the combination was blended with albendazole, processed using solvent-evaporation technique and adjuvant into a solid dispersion form (SD). The SD was granulated with starch and lubricated with magnesium stearate. Thermal analysis based on differential scanning calorimetry (DSC) and Fourier transmission infrared spectrophotometer (FT-IR) were carried out on the cellulose, drug and the granules. The micromeritic properties of the granules, and drug entrapment efficacy and dispersion-number of aqueous constitution of the granules were determined. The DSC result showed amorphous GC and granules. FT-IR analysis showed no compatibility or interaction problem based on the functional peaks observed. The granules exhibited micromeritics properties ($p > 0.05$); rate of consolidation < 0.43 and Carr's indices < 23.53, drug entrapment efficacy > 93 % and dispersion-number < 4.33. The granules dissolution rates after 10 and 60 mins were > 94.11 % and > 68.52 % respectively. These granules properties peaked with the GC and lactose combination at 20 % $^{w}/_{w}$ each. Albendazole formulation based on the cellulose obtained from sugarcane showed a promised alternative for improved dissolution and possible bioavailability enhancement.

Key: Solvent-evaporation, rate of consolidation, dispersion-number, dissolution-rate.

Introduction

Saccharum officinarum is the sugarcane plant with green tops, millable pseudostem, and roots. It is one of the two main species of genus Saccharum L. of Andropogoneae tribe of the grass family Poaceae (Schenck *et al*., 2004). *Saccharum officinarum* pseudostem is used to produce sugar and alcohol, leaving behind an abundant, non-toxic, stable, renewable, biocompatible and biodegradable sugarcane bagasse by-product (Cardona *et al*., 2010). About 50 % of the sugarcane bagasse is unused 50 % and is mainly made up of cellulose and soluble hemicellulose (Pandey *et al*., 2000). Sugarcane bagasse has been processed to xylose and different types of cellulose (Lavarack *et al*., 2000; Cerqueira *et al*., 2007; Mandal & Chakrabarty, 2011). Cellulose can be converted to nanocrystals, nanofibers, nanowhiskers and other forms using different processing techniques for different applications (Ejikeme, 2008; Akira & Bergstrom, 2014; Akira, 2018). Regeneration techniques that use combinations of different pure and aqueous

solutions at different stages have been used to convert natural cellulose to soluble cellulose derivatives with broadened application (Shabbir & Mohammad, 2017). The common application of the cellulose is its application in pharmaceutical formulation where the formulation scientists and the industrial pharmacy have recently focused their attention (Shabbir & Mohammad, 2017).

Pharmaceutically, improving the solubility of poor soluble drugs has been an ongoing study, and varied approaches have been evaluated. For instance, improving solubility characteristics of poorly soluble drugs using different strategies such as: specialised excipients, drug-excipient combinations, and formulation techniques have been used in drug dosage design.

First generation solid drug dispersion techniques spread out drug in solids that create eutectic solid dispersion with large surface areas, improved solubility and better drug release (Hallouard *et al*., 2016). On reconstitution with water this dispersion develops heightened molecular mobility that quickly solubilizes, but becomes unstable by quickly nucleating and re-crystallizing (Kramarczyk *et al*., 2023). To prevent the stability drawback of first generation solid dispersion, non-recrystallizing amorphous solid dispersions were formulated by dispersing amorphous solids in amorphous polymeric or homopolymeric carriers (Bhandare & Yadav, 2016; Kramarczyk *et al*., 2023). Amorphous solid can also be created if the rate of solidification of the molten or soluble solid and polymer blend is faster than the rate of alignment of their molecules into 3 dimensional crystal lattice order (Florence & Attwood, 2016; Jaiswar *et al*., 2016). Solvent evaporation formulation technique uses reduced hydration and heat stress conditions, and improved the rate of drying and cooling in creating this necessary condition for creating amorphous solid dispersion (Urbaniak & Musial, 2019). For this technique, physical mixtures of drug and excipients are dissolved in soluble volatile solvent and processed to properly blend before quickly evaporating and cooling the blend to leave solvent filmed solid dispersion (Urbaniak & Misial, 2019; Gupta *et al*., 2022). When dissolved in water, amorphous solid drug dispersions dissolve fast, do not crystallise promptly, retain their amorphous state and solubility advantages, and exhibit improved bioavailability (Florence & Attwood, 2016; Vasconcelos *et al*., 2021; Fukiage *et al., 2022;* Nnamani *et al*., 2022; Kramarczyk *et al.,* 2023).

The aim of this work is to formulate reconstitutable albendazole amorphous solid dispersion using generated cellulose from the bagasse of *Saccharum officinarum* pseudostem. Albendazole is a broad spectrum anthelmintic that disrupts the metabolic functions of parasites, and prevents them from replicating by killing and sterilising their eggs. Albendazole is a BCS class II drug with very poor aqueous solubility (< 0.01 mg / ml at 25 ℃) and good permeability (Yang *et al.*, 2021). Albendazole comes in different dosage forms and concentrations. Solid dosage forms of albendazole include chewable tablets and dry syrups for reconstitution (Kimaro *et al.,* 2019). The solubility and bioavailability of albendazole can be improved by converting albendazole to amorphous form and retaining / sustaining this amorphous form in solid formulation.

Materials and Methods

Materials

Albendazole powder (Hebei Qige Biotechnology Company Limited, Shijiazhuang, Hebei), Lactose (DEF Pharma, UK), corn starch (Bosida Starch Technology, Royi, Hohhot, China) and magnesium stearate (BOC Sciences Daily Chemical, Portland, London) powders were gifted from Dizpharm Limited. *Saccharum officinarum* pseudostem were harvested from the garden of Paxherbal and Laboratory Research, Ewu, Edo State. Analytical grade solvents were used.

Isolation and regeneration of cellulose from sugarcane pseudostem

Freshly harvested sugarcane was peeled of its hard waxy bark, desilicated, crushed into rough fibre using a hammer mill, and extracted of its juice using hot water, grinding and filtration. The fibrous residue from filtration (sugarcane bagasse) was depithed manually, and washed with excess deionized water and ethanol. Adapting the method of Shabbir and Mohammad (2017) for regeneration of cellulose, the sugarcane bagasse was immersed in 0.1N sodium hydroxide solution, heated to 110 ℃, and allowed to stand for 1 hr with constant stirring to pulp. The pulp was drained of water using filter cloth and immersed in 70 % ethanol to wash. The washed pulp was drained of ethanol and intensively washed with deionized water repeatedly twice. The isolated cellulose was immersed in a 5 L aqueous solution of 500 ml acetic acid and 50 ml nitric acid. The mixture was heated to 80 ℃ for 20 min, allowed to cool, and decanted. A 1 L aqueous solution of 20 g of sodium hydroxide and 50 ml of acetic acid was poured into the mixture, stirred for 10 min and filtered. The residue was washed intensively with deionized water and hand pressed using a filter cloth. The press was washed with 70 % ethanol and drained. The solid mass was washed thoroughly and repeatedly with deionized water, drained, pressed, and dried in a hot air oven at 112 ℃ for 30 min, and allowed to cool to dry mass. The dried mass was pulverised and sieved through a mesh size 25.

Organoleptic evaluation

The organoleptic properties of colour and smell were observed visually and by sniffing respectively.

Differential scanning calorimeter (DSC) analysis

Using 5.2 mg samples of generated cellulose, 1:1 generated cellulose in albendazole, and pure albendazole were used for DSC analysis. A sample was placed inside the curvet of PerkinElmer Differential Scanning Calorimeter (Model DSC 800, PerkinElmer Private Limited, India) set at left and right limits of 30 and 160 ℃ respectively. The readings of each test sample was read from an attached computer monitor and recorded.

Fourier transmission infrared (FT-IR) analysis

A 2 mg of generated cellulose, pure albendazole and 1:1 dispersion of albendazole in generated cellulose were measured separately as samples. A sample was made up to 200 mg with KBr, blended, pulverised and dried at 110 ℃ for 2 hours in a hot air oven. The dried blend was compressed to 80 mg pellet using a 13 mm diameter die and 8 tons of pressure for 3 min. FT-IR spectrum was recorded using the KBr disc on a Schimadzu FTIR-8400S Fourier transmission Infrared Spectrophotometer set at scan range of 4000 – 650 / cm with resolution of 4 / cm and 16 / cm. The FT-IR computer generated readings and spectra of the samples were printed out for analysis.

Preparation of albendazole solid dispersion.

Using 3^2 factorial design, 9 combinations of generated cellulose and albendazole active were factored out as expressed in table 1 for batches A-I. Using the adapted method of Fukiage *et al*. 2022 measures of albendazole, generated cellulose and cellulose for a batch were blended and milled using a Model LM2CB lab mixer with stainless steel base fitted with mesh 35. The sieved material was then mixed with 3 L of 3 / 1 $\frac{v}{v}$ acetone / absolute ethanol mixture in a stainless bowl and blended for 5 min using a stainless steel bowl stand mixer (Sokany Co., Zhejiang Province, China). The wet mass was dried at 80 ℃ for 10 min to obtain solid dispersion.

Preparation of albendazole pre-compression granules

The albendazole solid dispersion was blended with starchfor 2 min in the mixer, 2 ml hot water was poured into the mix while mixing for another 2 min to produce wet mass. The wet mass was passed through mesh 18. The resultant granules were spread

out on an aluminium tray and dried with hot air blow-gun drier at 80 ℃ for 10 min with constant turning to form dried granules. The dried granules were passed through mesh 14, and blended with fine magnesium stearate. The lubricated batch was weighed, filled into clean glass vials and labelled appropriately as batch A, B, C, D, E, F, G, H or I. The labelled vials were kept in a desiccator for 48 hrs before evaluation.

Table 1: Formula for albendazole granules

Excipients (g)	A	B	C	D	E	F	G	H	I
Albendazole	20	20	20	20	20	20	20	20	20
GC	6	12	18	12	18	6	18	6	12
Lactose	12	18	12	6	6	18	18	6	12
Starch	21.4	9.4	9.4	21.4	15.4	15.4	3.4	27.4	15.4
Magnesium stearate	0.6	0.6	0.6	0.6	0.6	0.6	0.6	0.6	0.6
Total (g)	60	60	60	60	60	60	60	60	60

Key: GC = Generated cellulose

Granules Yield values determination: % Granule yield

The weight of the granules obtained after preparation of the granules was used in calculating the percentage granules yield using equation 1 below.

$$\% \text{ granules yield} = \frac{actual\ weight\ of\ granules}{theoritical\ weight\ of\ granules} \quad \ldots\ldots 1$$

Drug loading and drug entrapment efficacy (DEE) determination

The method of Seifu *et al.* (2019) was adopted in determining DEE. A 600 mg granules from a batch was first transferred into a 100 ml volumetric flask and made to volume with acidified methanol. The resultant dispersion was sonicated for 120 sec using probe sonicator (PCI Analytics, Mumbai, India), and filtered. The filtrate was analysed for albendazole content using a UV/VIS spectrometer operation at 350 nm (Beckman 220 instruments, Fullerton, CA, USA). Using the method of Oyeniyi and Nnamani (2018), drug loading and drug entrapment efficacy were calculated from equations 2 & 3 below;

$$\text{Drug loading} = \frac{amount\ of\ drug\ in\ granules}{weight\ of\ granules} \quad \ldots\ldots 2$$

$$\text{Drug entrapment efficacy} = \frac{actual\ drug\ loaded}{theoretical\ drug\ loaded} \quad \ldots\ldots 3$$

Micromeritics evaluations

Micrometrics evaluations of the granuleswere done using particle arrangement and consolidation characterization. Adapting the method of Ilic *et al*. (2009) for particle rearrangement behaviour evaluation, a 10 g granules from a batch was poured through a funnel into 10 ml cylinder of 11.1 mm diameter and the outer of the cylinder tapped with the finger gently three time to mark (V_0). The cylinder was tapped on a padded wooden base from a height of 2.5 cm at the rate of 20 taps per minute in steps of 10 to 1000 taps. The tapped volumes (V_t) of the sample beds were recorded at 200, 400, 600, 800 and 1000 taps. The particle rearrangement parameters were used to estimate compactibility and

comprehension behaviours of the granules by applying Kawakita's densification parameters as stated by Ilic *et al.* (2009). The volume reduction ratio, C_N, of the dispersion was calculated using equation 4 below;

$$C_N = \frac{V_0 - V_t}{V_0} \quad \text{.....4}$$

Consolidation factor ($\frac{N}{C_N}$) was derived by dividing the number of taps by the volume reduction at the N tap. A plot of consolidation factor versus number of taps was made using Kawakita's densification equation (equation 5). The slope $\frac{1}{a}$ of the graph is use to estimate Carr's index, while $\frac{1}{b}$ is calculated from $\frac{1}{ab}$ y-intercept of the graph to estimate cohesiveness of powder.

$$\frac{N}{C_N} = \frac{1}{a} N + \frac{1}{ab} \quad \text{.....5}$$

The bulk density and tapped densities after N taps (calculated by dividing 10 g mass divided by respective bulk and tapped volumes) were applied in determining consolidation behaviours using Neumann consolidation equation (equation 6) as stated in Ogunjimi and Alebiowu (2013).

At N tap, Log ((Tapped density-Bulk density) / (Tapped density)) = K log N + C……..6

A graph of Log (Tapped density – Bulk density) / (Tapped density) plotted against Log N was used to derive an estimate of the rate of consolidation (K) from the slope and consolidation index (C) from y-intercept.

Aqueous dispersion characteristics: dispersion number

A 600 mg batch sample was weighed and poured into a cylinder. The cylinder was made up to 10 ml with de-ionized water and then stoppered firmly with a glass cork. The sealed cylinder was gently turned from standing position down 90 º and back, and observed for complete dispersion in water. The back and forth 90 º rotation was repeated, while counting, until complete dispersion is observed. The number of full turns needed for complete dispersion was recorded. The test was repeated three times, and the average number of turns recorded as dispersion number.

Drug release determination

Using a dialysis membrane tubing (80 – 100 kDa, Spectrum Inc., Lorzweiler, Germany) in acid pH 1.2 of hydrochloric acid, as a simulation of the release medium of the gastric juice, the in vitro release profile of albendazole granules were evaluated. A 120 mg granules (containing 40 mg albendazole) was enclosed in the dialysis membrane tubing and secured end-to-end with a thread. The membrane containing the granules was then suspended in 200 ml of hydrochloric acid solution (pH 1.2) in a beaker maintained at 37 ± 0.5 ℃ and set with mounted magnetic stirrer. The stirrer was rotated at 50 rpm and aliquots (5 ml) of the release medium were withdrawn at intervals and replaced with equal volume of fresh release medium to maintain sink conditions. The withdrawn samples were filtered and analysed at 350 nm wavelength in a UV-visible spectrophotometer. This experiment

was done in triplicates and the averages calculated for all the granuless.

Statistical analysis

Using the GC and Lactose from the 3^2 factorial design as variables and covariant, the test results from the granules were subjected to Microsoft Excel format statistical analysis. A 3 X 3 contingency table of GC and Lactose variables was used in the computation of Two-way ANOVA of the mean results in a design without repeated values.

Results

Organoleptic properties

The generated celluloses appeared off-white with no odour and no distinct taste.

DSC analysis

The differential scanning calorimetric (DSC) is presented in figure 1. The heat curve of the pre-treated cellulose had wide halo, the in transit isolated cellulose had narrow halo with sharp pointed end, while the transformed GC had wide halo. The fused solid dispersion showed a wide halo in their heat flow curves. The DSC curves of the fused 1:1 dispersion of albendazole in generated cellulose did not show any alteration of the exothermic or endothermic physical properties seen in the generated cellulose heat curve (Figure 1).

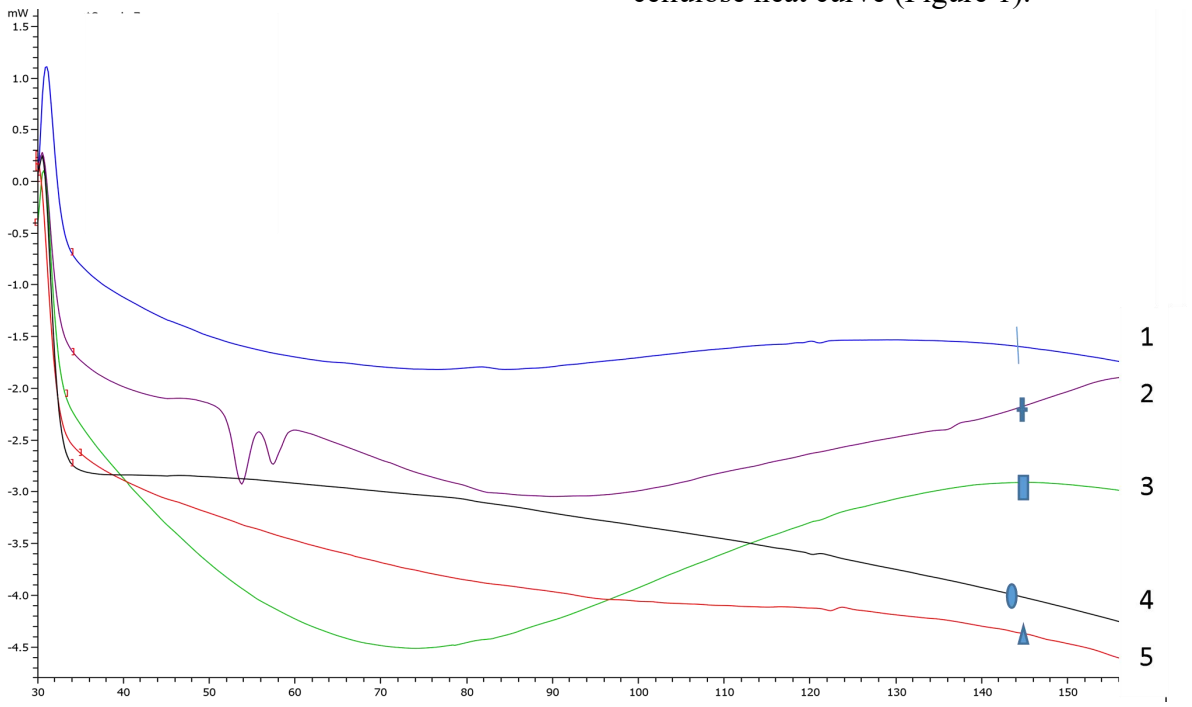

Figure 1: Differential scanning calorimetric graph of celluloses, solid dispersion of albendazole and albendazole.

Key:

1 = Generated sugarcane bagasse cellulose
2 = Isolated sugarcane bagasse cellulose
3 = Pre-treated sugarcane bagasse cellulose
4 = Albendazole
5 = 1:1 Solid dispersion of albendazole and sugarcane bagasse generated cellulose

FT-IR analysis

Fourier transmission infrared radiation (FT-IR) readings of the spectra scanned from 4000 to 650 / cm for GC, albendazole and fused dispersion of GC: albendazole are presented in figure. The FT-IR reading showed the presence of a broad transmission band of 3330 – 3390 /cm in all spectra in figure 2. The spectrum of fused dispersion of GC: albendazole maintained the peaks from the separate spectrum of albendazole and GC.

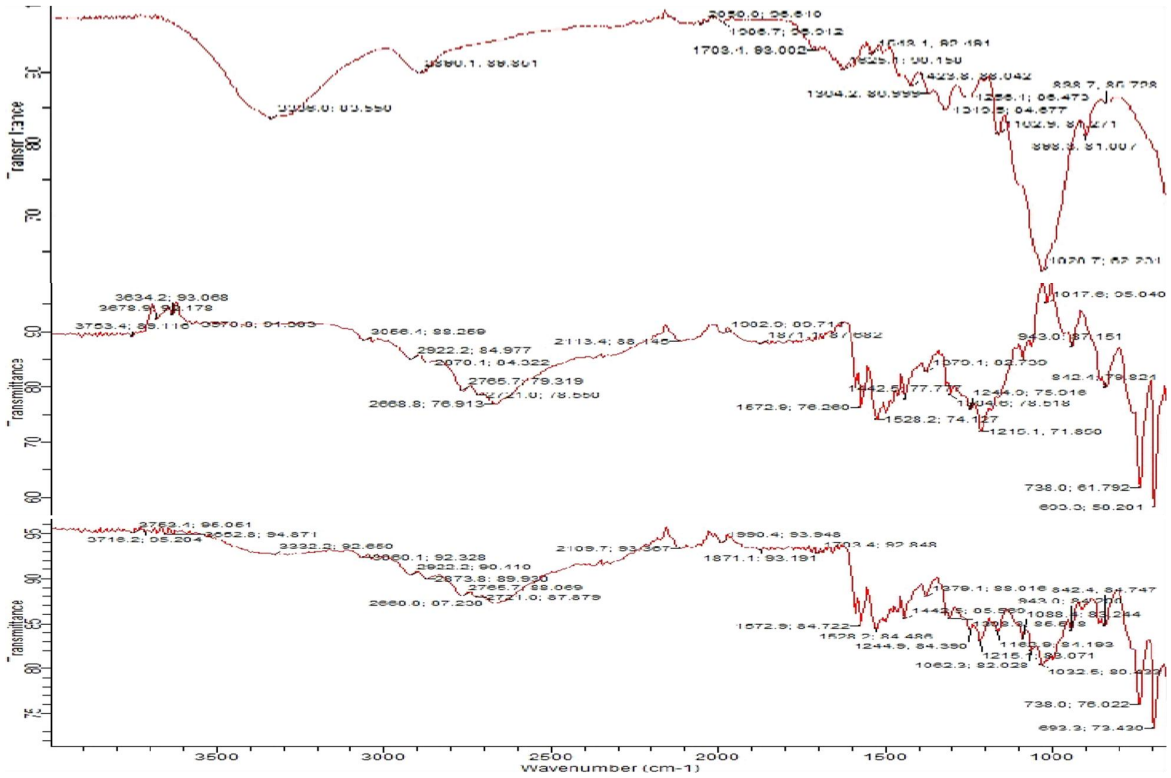

Figure 2 = FT-IR spectra of generated sugarcane bagasse cellulose, albendazole, and 1:1 dispersion of albendazole in generated cellulose

Yield values of granules

The percentage yield, drug loading (DL) and drug entrapment efficacy (DEE) values of the albendazole solid dispersion are presented in table 2. The % granules yield for the batches was 95.41 – 98.28 %. The drug loading and drug entrapment efficacies of the granules is presented in table 2. The DL of the batches is 33.33 %, while the DEE of the granules varied from 95.31 – 98.48 %.

Table 2: Content and yield values of granules

.	% GC	% Lactose	% Starch	DL (%)	G Yield (%)	DEE (%)
A	10.00	20.00	35.67	33.33	98.18	95.45 ± 1.18
B	20.00	30.00	15.67	33.33	97.45	95.31 ± 2.11
C	30.00	20.00	15.67	33.33	96.63	96.29 ± 2.76
D	20.00	10.00	35.67	33.33	98.28	96.54 ± 0.78

E	30.00	10.00	25.67	33.33	97.19	97.71 ±1.04
F	10.00	30.00	25.67	33.33	96.84	96.04 ± 2.97
G	30.00	30.00	5.67	33.33	95.41	98.98 ± 1.73
H	10.00	10.00	45.67	33.33	98.19	96.32 ± 0.96
I	20.00	20.00	25.67	33.33	97.22	96.11 ± 3.72

Key:
GC = generated cellulose. DL = drug loading. DEE = drug entrapment efficacy. G Yield = granules yield.

Micromeritic properties

The micromeritic properties of the granules are presented in table 3. The batches gave Kawakita's densification properties of maximum degree of compression range of 0.13 – 0.32, powder yield-strength range of 57.14 – 363.62, Carr's index range of 12.50 – 23.53, and consolidation index (c) and rate of consolidation ranges of -1.91 - -1.06 and 0.11-0.43 respectively. The graph of micrometrics properties is presented in figures 3 and 4, with batch B showing micrometrics flow and compaction characteristics with the most ascent in densification graph (Figure 3) and most descent in consolidation graph (figure 4).

Table 3: Micrometric properties of batches

.	a	1/b	Ca-I	K	C-I
A	0.18	33.33	17.65	0.11	-1.06
B	0.13	57.14	12.50	0.17	-1.39
C	0.22	139.53	18.75	0.27	-1.51
D	0.20	88.89	17.65	0.24	-1.44
E	0.22	225.02	17.65	0.31	-1.66
F	0.21	88.89	18.75	0.24	-1.42
G	0.32	363.62	23.53	0.43	-1.91
H	0.25	247.01	20.59	0.33	1.69
I	0.20	88.89	17.65	0.24	-1.44

Key:
a = maximum volume reduction
1/b = yield strength
Ca-I = Carr's index.
K = rate of consolidation.
C-I= consolidation index.

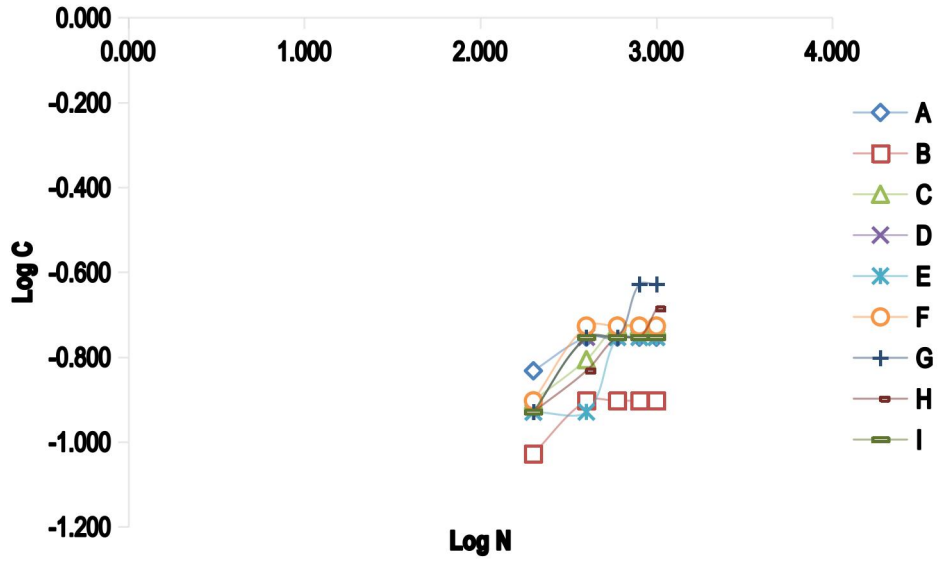

Key: C = consolidation index. N = Number of taps

Figure 3: Plot of consolidation behaviour of solid dispersion

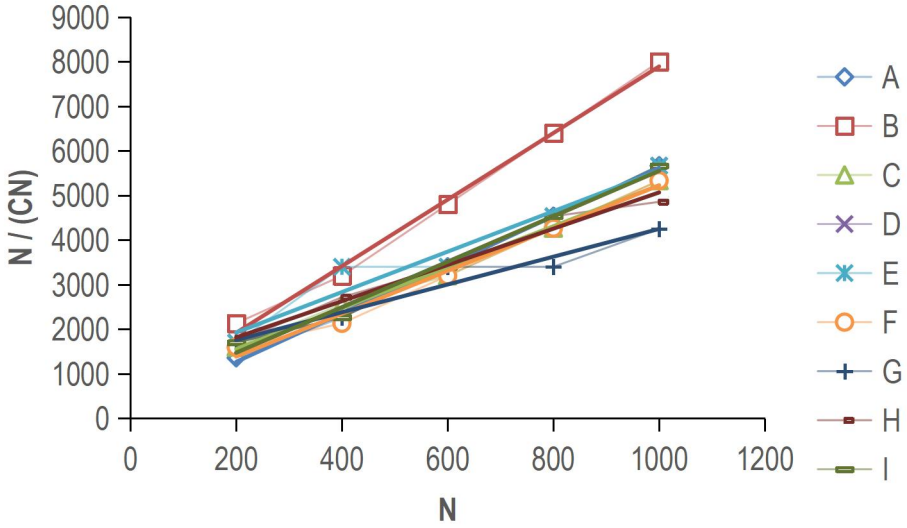

Key**:**
N = Number of taps
C_N = Powder volume reduction ratio
N / (C_N) = Powder consolidation factor
Figure 4: Plot of compressibility and compactibility behaviour

Aqueous dispersion characteristics: dispersion number.
The aqueous dispersion characteristics of the granules estimated from its dispersion number in aqueous medium is presented in table 4. The dispersion number range is 2.33 - 4.33.

Table 4: Drug release characteristics of albendazole granules

.	D-N	D_{T10}	D_{T60}
A	3.33 ± 0.47	94.45 ± 2.64	75.02 ± 2.64
B	3.67±	94.31 ±	74.5 ± 2.33

	0.47	3.91	
C	2.33± 0.47	96.29 ± 3.47	81.16 ± 3.91
D	3.67± 0.47	93.54 ± 2.12	68.52 ± 1.64
E	2.67± 0.47	97.71 ± 2.33	78.56 ± 2.64
F	4.33± 0.47	96.04 ± 4.18	74.01 ± 1.64
G	2.00± 0.00	98.48 ± 2.13	84.71 ± 3.89
H	4.33± 0.47	95.38 ± 3.11	74.29 ± 2.34
I	3.67± 0.47	94.11 ± 2.14	74.91 ± 1.78

Key:
D_{T10} = Drug released in dissolution medium after 15 min
D_{T60} = Drug released in dissolution medium after 60 min
D-N = number of turns required to achieve complete dispersion

Drug release properties

The drug dissolution profile of the albendazole granules is presented in Figure 5. The batches C, E and G showed highest dissolution after 30 min, and least decline in dissolution after 60 min.

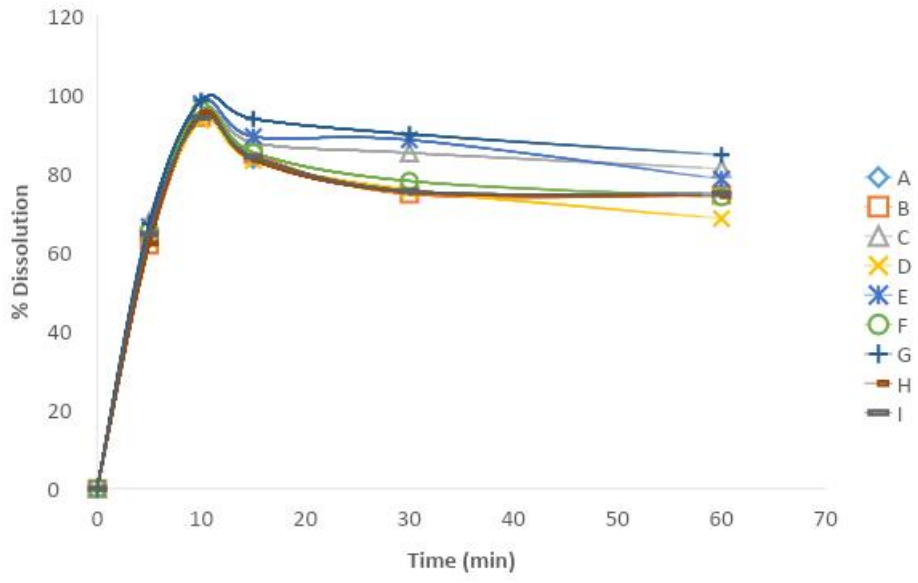

Figure 5: Dissolution profile of albendazole solid dispersion

Statistics analysis

The statistical analysis showed that the difference between the GC concentrations is insignificant to the DEE at 5 % level. The statistical analysis showed that the difference between the GC concentrations is insignificant to dissolution at 15 min but significant to dissolution at 60 min.

Discussion

An off-white colour, odourless and tasteless pharmaceutical grade excipient properties developed from cellulose regeneration are suitable organoleptic properties for drug adjuncts. The <1.23 Hausner ratio and <20 Carr's index is an indication of improved fair flow rate (Maheshwari *et al*., 2018). The absence of sharp melting point in DSC curves for generated cellulose and albendazole solid dispersion is indicative of amorphous material. Florence and Attwood (2016) had described amorphous materials as having no sharp melting point. The albendazole remained compatible with the generated cellulose, retaining its heat behaviour. The FT-IR reading of the generated cellulose showed that the chemical structure of cellulose is intact after regeneration. The presence of broad transmission band of 3330 – 3390 /cm in GC spectrum falls within the 3500 -3200 /cm of O-H stretching vibration of hydroxyl group absorption of water present in cellulose that is consistent with description of cellulose from Sain and Panthapulakkal (2006) and Kumer *et al*. (2013). The peak absorption at 2900 / cm for GC spectra is consistent with peak absorption range of cellulose stated in Shanmugam *et al.* (2015). The presence of 2873-2898 / cm band is due to C-H stretching of aryl groups aliphatic bonds of cellulose as described in Sheltami *et al*. (2012). While the absence of 1760-1650 of C-O stretching band is due to cleavage of acetyl, uronic and other ester linked substances of hemicellulose and lignin due to alkali treatment of bagasse similar to descriptions by Mandal and Chakraberty (2011) and Lu and Hsieh (2012). The absence of the 1508-1447 band is due to removal of lignin from cellulose inferred from the description of Sheltami *et al*. (2012). The presence of 1430-1420 band is due to CH_2 scissors vibration motion of cellulose. The 1045 / cm and 1105 / cm bands are due to the C-O-C pyranose ring and C-O-C glycosidic ether bonds are shown by the 1150 / cm band. The cellulosic β- glycosidic linkage is shown by the presence of 902 – 893 / cm band following the observation from Pandey *et al.* (2000) are shown, and are unaffected in the GC spectrum. The inference is that no new compound was formed from cellulose regeneration (Hinterstoisser & Salmen, 2000). The FT-IR spectra of the solid dispersion of albendazole in GC showed a merger of the spectra of GC and albendazole with no new peak or trough. The inference is that the albendazole formulation was formed from the solid dispersion and granules formation.

The micromeritics properties of the batches showed passable flow properties with good consolidation, compression and compactibility properties. All the batches had Carr's indices < 0.23, a value which in Ogunjimi and Alebiowu (2013) is indicative passable powder flow. The yield strength (1/b), which is the pressure needed for powder to reach half of maximum volume reduction or the cohesive energy of powder interaction which resists particle rearrangement, were > 33.33. This high yield strength increases with GC concentration. High yield strength, from study of Ilic *et* al. (2019), is an indication of compactable and compressible non-plastic powder. Powders that require high pressure to compress often form hard compacts (Persson *et al*., 2022). The flow properties of albendazole granules reduces with increase in GC concentration and conforms to findings by Szabo *et* al. (2019) that granules have poor flowability properties. These non-plastic behaviour and consolidation characteristics are indicative of metastable powders that have not experienced unwanted microstructural coarsening nor changes as stated by Groza (2007).

The rate of dispersion of reconstituted granules in water increases with increase in GC concentration. This result is in line with findings by Kramarczyk *et al*. (2023) concerning solubility and amorphousness. Florence and Attwood (2016) agrees with the increase in solubility of amorphous

solids. Earlier works such as by Azad *et* al. (2018) showed that albendazole solid dispersions had better dissolution properties. The stability of the granules in aqueous solution was evident by the presence of over > 68.52 % albendazole in the dissolution medium after 60 min. This decrease in Albendazole content in the dissolution medium can be attributed to recrystallization of some dissolved albendazole molecule. This results agrees with reports by Kramarczyk *et al*. (2023) on recrystallization of drugs with time in dissolution medium. In this study, the higher the GC, the lower the loss in albendazole after 60 min. This is indicative of the stabilising effect of GC polymer on granules. The stability and % dissolution of albendazole granules increased with increase in concentration of GC in the granules.

Conclusion

The stepwise isolation, pre-treatment and regeneration of sugarcane bagasse cellulose produced soluble amorphous generated cellulose that is chemically compatible with albendazole. The dispersion of albendazole in the generated cellulose produced amorphous solid dispersion. The amorphous solid dispersion of albendazole had good compressibility and non-plastic behaviour suitable for filling and compaction. The compaction properties of amorphous solid dispersion increased with increase in generated cellulose polymer content. The amorphous dispersion dissolved fast in water at a rate proportional to generated polymer cellulose content. After about 30 min, the albendazole content in the aqueous medium begins to decrease at a rate that is inverse to its generated polymer cellulose content. Formulation of albendazole drug in amorphous solid dispersion with generated cellulose and lactose improved the compactability, solubility and stability properties of albendazole solid dosage form. While the lactose concentration was responsible for quick onset dissolution, the GC and lactose solid dispersion combination was responsible for stabilizing the albendazole amorphous solid dispersion. This improvement in dosage form and drug delivery is optimal when 33.33 percent albendazole is dispersed in 60 percent of 1:1 generated cellulose / lactose carrier polymer. Further research may bring up other pharmaceutical dosage design applications of processed sugarcane bagasse.

Acknowledgment

We are grateful to the Department of Pharmaceutics and Pharmaceutical Technology, Dora Akunyili College of Pharmacy, Igbinedion University Laboratory staff that assisted in sugarcane bagasse extraction. We are grateful to Igbinedion University IT unit that provided seminars on statistical computation and digital applications. We are grateful to Ahmadu Bello University Research centre for allowing us to use their FT-IR and DSC analyser machines.

Conflict of interest

There is no conflict of interest. No external financial support was obtained.

References

Akira I (2018). Development of completely dispersed cellulose nanofibers. Proceedings of the Japan Academy Series B, Physical and Biological Sciences 94(4): 161-179.

Akira I, Bergstrom L (2014). Preparation of cellulose nanofibers using green and sustainable chemistry. Current Opinion in Green and Sustainable Chemistry, 12: 15-21. Doi.org/10.1016/j.cogsc.2018.04.008.

Azad AK, Jahan K, Sathi TS, Sultana R, Abbas SA, Uddin AH (2018). Improvement of dissolution properties of albendazole from different methods of solid dispersion. Journal of Drug Delivery and Therapeutics, 8(5): 475-480. Doi:http://dx.doi.org/10.22270/jddt.v8i5.1942.

Bhandare PS, Yadav A (2016). A review on dry syrup for paediatrics. International Journal of Current Pharmaceutical Research, 9(1): 25-31. Doi:10.22159/ijcpr.2017v9i1.16789.

Cardona CA, Quintero IC, Paz IC (2010). Production of bioethanol from sugarcane bagasse: status and perspectives. Bioresource Technology, 101: 4754-4766.

Cerqueira DA, Guimes RF, Carla da SM (2007). Optimization of sugarcane bagasse cellulose acetylation. Carbohydrate Polymer, 69: 579-582.

Ejikeme PD (2008). Investigation of the physicochemical properties of microcrystalline cellulose from agricultural wastes I: orange mesocarp. Cellulose, 15: 141-147.

Florence AT, Attwood D (2016). Solids in Physicochemical Principles of Pharmacy: In Manufacture, Formulation and Clinical Use 6th ed. Pharmaceutical Press, Smithfield, London. Chp , pp 7- 68.

Fukiage M, Suzuki K, Matsuda M, Nishida Y, Oikawa M, Fujita T, Kawakami K (2022). Inhibition of liquid-liquid phase separation for breaking the solubility barrier of amorphous solid dispersion to improve oral absorption of naftopidil. Pharmaceutics, 14: 2664-2679. https://doi.org/10.3390/pharmaceutics14122664.

Groza JR (2007). Nanocrystalline powder consolidation methods In Nanostructured Materials (2nd edtn.) William Andrew Publishing. Chp 5, pg 173-233. https://doi.org/10.1016/B978-081551534-0.50007-5.

Gupta MS, Gowda DV, Kumar TP, Rosenholm JM (2022). A comprehensive review of patented technologies to fabricate oral dispersible films: proof of patent analysis (2000-2020) (2022). Pharmaceutics 14:820. https://doi.org/10.3390/pharmaceutics14040820.

Hallouard F, Mehenmi L, Malika L-S, Anouar Y, Skiba M (2016). Solid dispersion for oral administration: an overview of the methods for their preparation. Current Pharmaceutical Design 22(32): 1-17 doi:10.2174/1381612822666160726095916.

Hinterstoisser B, Salmen L (2000). Application of dynamic 2D FT-IR to cellulose. Vibrational Spectroscopy, 22: 111-118.

Ilic IG, Kasa Jr PK, Dreu R, Pintye-Hodi K, Srcic S (2009). The cpmpressibility and compactibility of different types of lactose. Drug Development and Industrial Pharmacy, 35(10):1271-1280. http://www.tandfonline.com/doi/full/10.1080/03639040902932945.

Jaiswar DR, Jha D, Amin PD (2016). Preparation and characterizations of stable amorphous solid solution of azithromycin by hot-melt extrusion. Journal of Pharmaceutical Investigation 46, 655-668. https://doi.org/10.1007/s40005-016-0248-x.

Kimaro E, Tibalinda P., Shedafa R., Temu M. and Kaale E. (2019). Formulation development of chewable albendazole tablets with improved dissolution rate. Heliyon, e02911 1-8.

Kramarczyk D, Knapik-Kowalczuk J, Kurek M, Jamroz W, Jachowicz R, Paluch M (2023). Hot melt extruded posacinazole-based amorphous solid dispersions- The effect of different types of polymers. Pharmaceutics 15: 799-821. https://doi.org/10.3390/pharmaceutics15030799.

Lavarack BP, Griffin GJ, Rodman D (2000). Measured kinetics of the acid-catalysed hydrolysis of sugarcane bagasse to produce xylose. Catalysis Today, 63(2-4): 257-265.

Lu P, Hsieh Y (2012). Cellulose isolation and core-shell nanostructure of cellulose nanocrystals from Chardonnay grape skins. Carbohydrate Polymers, 87: 2546-2553.

Maheshwari R, Todke P, Kuche K, Raval N, Tekade RK (2014). Micromeritic in pharmaceutical product development. In Tekade, R. K (ed), Dosage Design Considerations. Associated Press 17, pp 599-626. Elsevier Inc. Doi; https://doi.org/10.1016/B9778-0-12-814423-7.00017-4.

Mandal A, Chakrabarty D (2011). Isolation of nanocellulose from waste sugarcane bagasse (SCB) and its characterization. Carbohydrate Polymers, 86: 1291-1299.

Nnamani ND, Onaga IC, Esezobo S (2022). A comparison of physicochemical properties of high drug-loaded tablets formulated with cold gelatin gummies. Journal of Pharmaceutical and Allied Sciences, 19(3): 3769-3780.

Oginjimi A, Alebiowu G (2013). Flow and consolidation properties of neem gum coprocessed with two pharmaceutical excipients. Poweder Technology, 246: 187-192. Doi:10.1016/j.powtec.2013.04.051.

Oyeniyi YJ, Nnamani ND (2018). Preparation and evaluation of 5-fluoracil solid dispersion formulations for therapeutic management of colorectal cancer (CRC). African Journal of Pharmaceutical Research and Development, 10(2): 127-134.

Pandey A, Soccol C, Nigam, P Soccol V (2000). Biotechnological potential of agro-industrial residues. I: sugarcane bagasse. Bioresources Technology, 74: 69–80.

Persson A-S, Pazesh S, Alderborn G (2022). Tabletability and compactibility of α-lactose monohydrate powders of different particle size. 1. Experimental comparison. Pharmaceutical Development and Technology, 27: 1-12 https://doi.org/10.1080/10837450.2022.2051550.

Sain M, Panthapulakkal S (2006). Bioprocess preparation of wheat straw fibers and their characterization. Industrial Crops and Products, 23: 1-8.

Seifu A, Kebede E, Bacha B, Melaku A, Setegn T (2019). Quality of albendazole tablets legally circulating in the pharmaceutical markets of Addis Adaba, Ethiopia: physicochemical evaluation. BMC Pharmacol Toxicol, 20: 20. Doi: 10.1186/s40360-019-0299-5.

Schenck S, Crepeau MW, Wu KK, Moore PH, Yu Q (2004). Genetic diversity and relationships in native Hawaiian Saccharum officinarum sugarcane. Journal of Heredity 95(4):327-331.

Shabbir M, Mohammad F (2017). Sustainable production of regenerated cellulosic fibres. The Textile Institute Book Series. Pg 171 – 189. https://doi.org/10.1016/B978-0-08-102041-8.00007-X.

Shanmugam N, Nagarka RD, Kurdhade M (2015). Microcrytalline cellulose powder from banana pseudostem fibres using biochemical route. Indian Journal of Natural Products and Resources, 6(1): 42-50.

Sheltami R, Abdullah I, Ahmada I, Dufresne A, Kargarzadeh H (2012). Extraction of cellulose nanocrystals from Mengkuang leaves (Pandanus tectorius). Carbohydrate Polymers 88: 772-779.

Szabo E, Demuth B, Galata DL, Vass P, Hirsch E, Csontos I, Marosi G, Nagy ZK (2019). Continuous formulation approaches of amorphous solid dispersions: significance of powder flow properties and feeding performance. Pharmaceutics 11(12): 654. Doi:10.3390/pharmaceutics11120654.

Urbaniak T, Musial W (2019). Influence of solvent evaporation technique parameters on diameter of submicron lamivudine-poly-ε-caprolactone conjugate particles. Nanomaterials (Basel), 9(9): 1240. Doi:10.3390/nano9091240.

Vasconcelos T, Prezotti F, Araujo F, Lopes C, Loureiro A, Marques S, Sarmento B (2021).. Third-generation solid dispersion combining soluplus and poloxamer 407 enhances the oral bioavailability of resveratrol. International Journal of Pharmaceutics, vol 595, 120245. https://doi.org/10.1016/ijpharm.2021.120245.

Yang Z-Z, Fan G-Q, Zhang T-T, Li D-B, Pei L-L, Huang R-Y, Yin D-P, Zhang L, Peng G-N, Shu G, Yuan Z-X, Lin J-C, Zhnag W, Zhong Z-J, Yin L-Z, Fu H-L (2021). Determination of solubility and thermodynamic properties of albendazole in binary solvent of ethanol and water. Physics and Chemistry of Liquids, 59:1, 1-11, doi:10.1080/00319104.2019.1660979.